Two nucleon knockout from ^{4}He using a translationally invariant wavefunction

W. Van Nespen[1,†] and J. Ryckebusch[1]

[1] *Department of Subatomic and Radiation Physics, Ghent University, Belgium*

Recently, a lot of experimental and theoretical efforts have been directed into the study of short-range correlations (SRC) in nuclei. Experiments with a dense nuclear target like ^{4}He are expected to maximize the signals of SRC in the physical observables. We outline a plane-wave model for calculating observables of electromagnetically induced two-nucleon knockout processes from ^{4}He and present some preliminary results of $^4\mathrm{He}(\gamma, pp)nn$ and $^4\mathrm{He}(e, e'pp)nn$ calculations.

1. INTRODUCTION

From experiments involving real and virtual photons, a lot of evidence has been accumulated which advocates the use of a more profound description of the nuclear interior than provided by the independent particle model (IPM). For example, the IPM does not account for the small spectroscopic factors which are extracted from $\mathrm{A}(e, e'p)$ measurements. One frequently adopted technique to go beyond the IPM is the correlated-basis function approach (CBF). In this approach, the IPM wavefunction is multiplied by a series of ascending powers in the central correlation function. One of the ongoing nuclear physics research goals is to try to pin down the effect of short range correlations in nuclei. Due to its high central density (almost three times nuclear matter density) the helium nucleus is a particularly appropriate system to search for signs of the SRC. An appropriate tool to probe the SRC is the two-nucleon knockout reaction initiated by the electromagnetic force. Unfortunately, apart from SRC also other reaction mechanisms contribute to the two-nucleon knockout process. A genuine signature of SRC is for example a fast forward going nucleon accompanied by a backward going nucleon while the residual two-body system has almost zero recoil momentum.

The theoretical models which are typically used for modeling two-nucleon knockout from medium and heavy nuclei are subject to major modifications when going to lighter nuclear targets. After the ejection of two nucleons from "heavy" nuclei (^{12}C, ^{16}O $\cdots$) the residual nucleus can be assumed to be captured in more or less the same potential as the target one and does not gain large amounts of recoil momentum. Light nuclei, on the other hand, require a different approach which treats the recoil effects correctly. Recoil effects occur on the kinematical as well as on the dynamical level and give rise to so-called recoil diagrams in the description of the reaction process. Recently, some groups have computed realistic and translationally invariant ground state wavefunctions for ^{4}He. A detailed review of these efforts can be found in Refs. [1] and [2]. These days, a major fraction of the experimental efforts to probe SRC effects in nuclei is concentrated on lighter nuclei. A $^4\mathrm{He}(e, e'pp)nn$ experiment has been performed at the ELSA facility in Bonn [3] while in the near future $^4\mathrm{He}(\vec{\gamma}, pp)nn$ and $^4\mathrm{He}(\vec{\gamma}, pn)X$ data from the PIP-TOF collaboration in Mainz will become available [4].

In Section II a plane-wave model for the description of electromagnetically induced two-nucleon knockout from ^{4}He will be described. In section III some preliminary results of exclusive $^4\mathrm{He}(e, e'pp)nn$ and $^4\mathrm{He}(\vec{\gamma}, pp)nn$ calculations will be presented. Our conclusions and prospects will be summarized in Section IV.

2. A TRANSLATIONALLY-INVARIANT MODEL FOR TWO-NUCLEON KNOCKOUT

Our calculations are performed in so-called coplanar (see Fig 1) kinematics adopting a plane wave description for the ejected particles.

[†] Electronic address: wim.vannespen@rug.ac.be

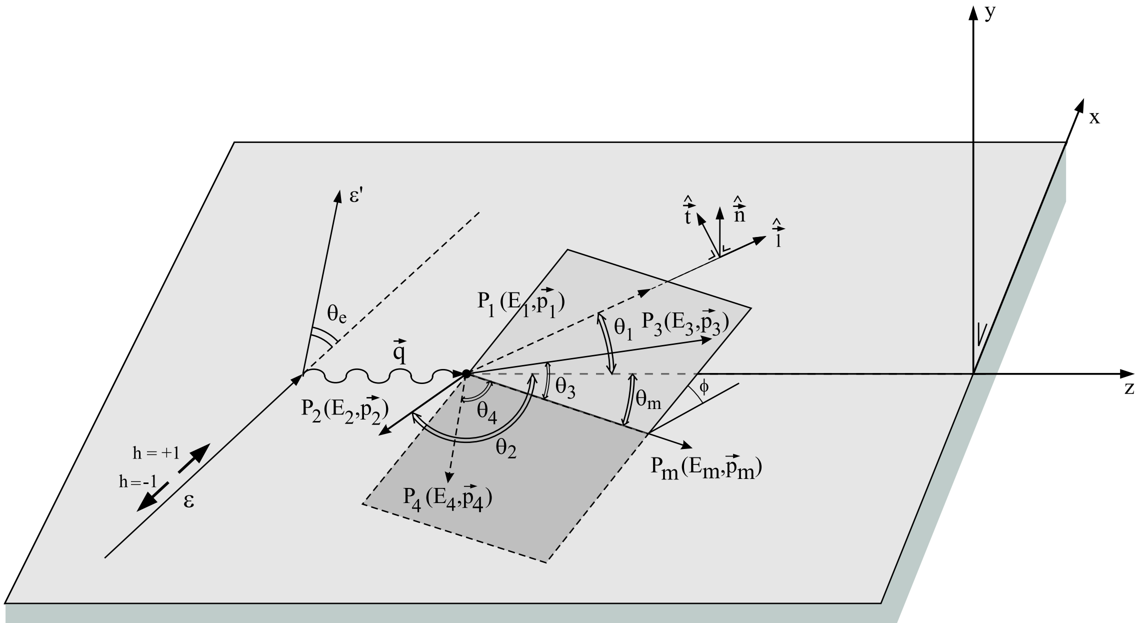

FIG. 1: Kinematical variables for the ^{4}He$(e, e'NN)NN$ reaction in a coplanar kinematics.

The ^{4}He wavefunction which has been used in the numerical calculations has the following structure :

$$\Psi_{^4He} = \mathcal{S} \prod_{i<j=1}^{4} (1 + u_{t\tau}(\vec{r}_{ij})(3\frac{\vec{\sigma}_i.\vec{r}_{ij}\vec{\sigma}_j.\vec{r}_{ij}}{r_{ij}^2} - \vec{\sigma}_i.\vec{\sigma}_j)) \prod_{k<l=1}^{4} f_c(\vec{r}_{ij}) \Phi_{S=0,T=0} \ , \tag{1}$$

with $\Phi_{S=0,T=0}$ a spin-isospin Slater determinant and $\mathcal{S}$ the symmetrizing operator. Note that in contrast to the standard CBF approach the reference Slater determinant contains only the spin-isospin parts of the IPM wavefunctions, a procedure which ensures that the total wavefunction has the correct asymptotic behaviour. The latter approach returns a translationally invariant wavefunction. The central correlations, though, constitute an essential part of the wavefunction while for the tensor correlation part a cluster expansion can be justified :

$$\Psi_{^4He} \approx \left(1 + \sum_{i<j=1}^{4} u_{t\tau}(\vec{r}_{ij})(3\frac{\vec{\sigma}_i.\vec{r}_{ij}\vec{\sigma}_j.\vec{r}_{ij}}{r_{ij}^2} - \vec{\sigma}_i.\vec{\sigma}_j) + \cdots \right) \prod_{k<l=1}^{4} f_c(\vec{r}_{ij}) \Phi_{S=0,T=0} \ .$$

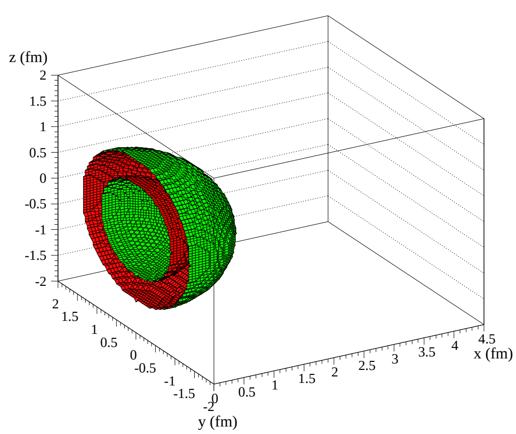

FIG. 2: Equiprobability surface for the inter-particle separation distribution in ^{4}He.

We use the correlation functions as they were determined by means of a Greens Function Variational Monte Carlo (GFMC) technique developed by the Argonne-Urbana group [2].

To keep computational times within reasonable ranges, the tensor correlations have been neglected in our two-nucleon knockout calculations. Fig 2 displays an equiprobability surface for the inter-nucleon separation distribution in ^{4}He. This surface is the locus of all points with the same probability (here, P = 10 %) to find two nucleons at a certain inter-particle distance defined by the

coordinates (x, y, z). As becomes obvious from this picture, the presence of the SRC pushes the nucleons out of each others vicinity creating a dumbbell shape [5] in the internucleon density distribution which corresponds with the creation of some forbidden region around each nucleon.

Another well-known consequence of the presence of SRC becomes apparent in the momentum distribution. Fig. 3 shows the one-particle momentum distribution. One observes how the SRC shift strength from the low- to the high-momentum region. A full scale calculation for the momentum distribution, including tensor correlations up to all orders, has been performed by the Argonne-Urbana group and is shown by the red triangles [9] . The tensor correlations are observed to enhance the momentum distribution at intermediate momenta.

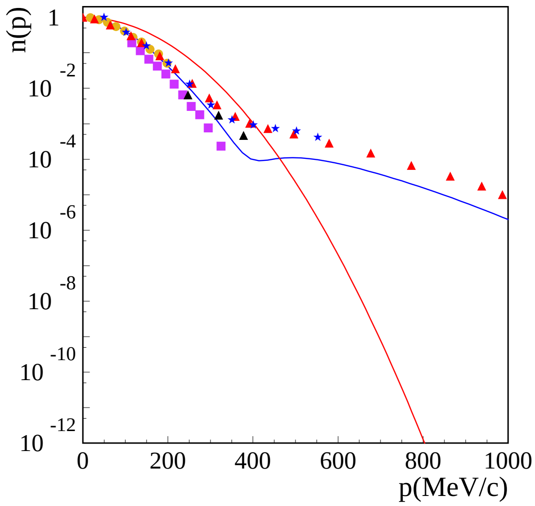

FIG. 3: One-body momentum distribution for ^{4}He. The red curve has been obtained using an harmonic oscillator wavefunction while the blue curve is the realistic calculation using the wavefunction from Eq. 1 without tensor correlations. The brown dots, purple squares and black triangles are data sets from Refs. [6] and [7] respectively. The blue stars have been extracted from the experimental spectral function in a model-dependent way as explained in Ref. [8].

The expression for the $(e, e'pp)$ cross-section reads:

$$\frac{d^9\sigma}{d|\vec{k}_1|d\Omega_1 d|\vec{k}_2|d\Omega_2 d|\vec{k}_{e'}|d\Omega_{e'}}(\vec{e}, e'\vec{p}p) = \frac{1}{\hbar c}\frac{1}{(2\pi)^9}\left(\frac{d\sigma}{d\Omega_{e'}}\right)_{\mathrm{M}} \int_\Omega |\vec{k}_1|^2 |\vec{k}_2|^2 |\vec{k}_3| E_3 f_{\mathrm{rec}}^{-1}$$
$$\times \left\{ v_L W_L + v_T W_T + v_{LT} W_{LT} + v_{TT} W_{TT} + h \left(v'_{LT} W'_{LT} + v'_{TT} W'_{TT} \right) \right\} d\Omega_3 \; .$$

The $v_L, v_T, v_{LT}, v_{TT}, v'_{LT}$ and v'_{TT} depend solely on the electron kinematics while the structure functions $W_L, W_T, W_{LT}, W_{TT}, W'_{LT}$ and W'_{TT} are determined by the nuclear current operator and the structure of the initial and final wave function. For a circularly polarized real photon only the W_T and W'_{TT} survive while for a linearly polarized photon the observables are determined in terms of the W_T and W_{TT}. Additional information with respect to the different reaction mechanisms could be obtained by studying the photon asymmetry, the recoil and induced polarization observables. Due to Lorentz and parity invariance some of the polarization observables become identical to zero when performing the calculations in coplanar kinematics [10]. In the plane wave approximation, of all induced and polarization transfer observables only two give non-vanishing numbers (i.e. P'_l, P'_t) :

$$P'_{i(=l,t)} = \frac{\left[d^9\sigma(h=1, s_i^1 \uparrow) - d^9\sigma(h=-1, s_i^1 \uparrow)\right] - \left[d^9\sigma(h=1, s_i^1 \downarrow) - d^9\sigma(h=-1, s_i^1 \downarrow)\right]}{\left[d^9\sigma(h=1, s_i^1 \uparrow) + d^9\sigma(h=-1, s_i^1 \uparrow)\right] + \left[d^9\sigma(h=1, s_i^1 \downarrow) + d^9\sigma(h=-1, s_i^1 \downarrow)\right]} \; ,$$

while in the real photon case (linearly polarized) only the photon asymmetry (Σ) survives as an experimentally accessible quantity :

$$\Sigma = \frac{d^9\sigma_\parallel - d^9\sigma_\perp}{d^9\sigma_\parallel + d^9\sigma_\perp} \; .$$

The photon asymmetry (Σ) [11] and the nucleon transfer polarizations (P'_l, P'_t) [12] are well-known to be rather insensitive to effects from the final-state interactions which make them a particularly promising tool to study the effects of SRC.

In our calculations, we use plane waves to describe the ejected nucleons. To eliminate the spurious contributions to the scattering matrix a Gramm-Schmidt orthogonalization procedure was adopted. The nuclear current operator has been derived on the basis of an effective Lagrangian

approach. Apart from a one-body part it contains pion exchange and delta excitation diagrams. The one-body current is the common lowest-order relativistic reduction of the Dirac current and contains a convection and magnetization term. These currents have the well-known form :

$$\rho_{L.O.} = e G_E^p(Q^2) \frac{1+\tau_z}{2} \,,$$
$$\vec{J}_{L.O.} = e \frac{G_E^p(Q^2)}{2m_N} (\vec{p}' + \vec{p}) \frac{1+\tau_z}{2} + e \frac{i}{2m_N} \left[G_M^p(Q^2) \frac{1+\tau_z}{2} + G_M^n(Q^2) \frac{1-\tau_z}{2} \right] \vec{\sigma} \times \vec{q} \,.$$

To be consistent with the long range part of the Argonne v_{18} potential, which consists entirely of one-pion exchange, we incorporated the pion exchange diagrams into the nuclear current. The pion exchange current is composed of the pion seagull and pion in-flight diagrams :

$$\vec{J}_{\rm seagull} = -ie \left(\frac{f_{\pi NN}^{PV}}{m_\pi} \right)^2 (\vec{\tau}_1 \times \vec{\tau}_2)_z \left[\vec{\sigma}_1 \frac{\vec{\sigma}_2 . \vec{k}_2}{|\vec{k}_2|^2 + m_\pi^2} - \frac{\vec{\sigma}_1 . \vec{k}_1}{|\vec{k}_1|^2 + m_\pi^2} \vec{\sigma}_2 \right] \,,$$
$$\vec{J}_{\rm in\text{-}flight} = -ie \left(\frac{f_{\pi NN}^{PV}}{m_\pi} \right)^2 (\vec{\tau}_1 \times \vec{\tau}_2)_z \frac{\vec{\sigma}_1 . \vec{k}_1}{|\vec{k}_1|^2 + m_\pi^2} \frac{\vec{\sigma}_2 . \vec{k}_2}{|\vec{k}_2|^2 + m_\pi^2} \left[\vec{k}_2 - \vec{k}_1 \right] \,,$$

where, $\vec{k}_i = \vec{p'}_i - \vec{p}_i$.
Hadronic formfactors of the monopole form have been introduced at the meson-baryon vertices. Gauge invariance is violated as soon as one introduces hadronic formfactors as well as when the current operator is not directly derived from the effective nucleon-nucleon force used to determine the wave functions. We adopt the common technique for restoring gauge invariance and replace the third component of the current by the charge operator ($\vec{J}_z \rightarrow \frac{\omega}{|\vec{q}|} \rho$). From $(e, e'NN)$ and (γ, NN) calculations for medium and heavy nuclei [13] it became clear that the delta current is a very essential ingredient of the two-nucleon knockout process. Actually, in a wide energy range about the Δ resonance peak it turned out to be the dominant reaction mechanism. The non-static Δ-current operator which we use reads:

$$\begin{aligned} \vec{J}_{\rm delta} = ie \frac{1}{9} \frac{f_{\pi NN}^{PV} f_{\pi N\Delta} f_{\gamma N\Delta}}{m_\pi^3} G_{\gamma N\Delta}(Q^2) \Bigg\{ & \left[G_\Delta^{res} + G_\Delta^{non-res} \right] \frac{\vec{\sigma}_2 . \vec{k}_2}{|\vec{k}_2|^2 + m_\pi^2} \\ & \times \left(4(\tau_2)_z \vec{k}_2 \times \vec{q} - (\vec{\tau}_1 \times \vec{\tau}_2)_z (\vec{\sigma}_1 \times \vec{k}_2) \times \vec{q} \right) + \\ & \left[G_\Delta^{res} - G_\Delta^{non-res} \right] \frac{\vec{\sigma}_2 . \vec{k}_2}{|\vec{k}_2|^2 + m_\pi^2} \\ & \times \left(-2i(\tau_2)_z (\vec{\sigma}_1 \times \vec{k}_2) \times \vec{q} - 2i (\vec{\tau}_1 \times \vec{\tau}_2)_z \vec{k}_2 \times \vec{q} \right) + 1 \leftrightarrow 2 \Bigg\} \,, \end{aligned}$$

where G_Δ^{res} and $G_\Delta^{non-res}$ are the delta propagators for resonant (s-channel) and non-resonant (u-channel) excitation respectively. Both propagators depend on the Mandelstam variable s. More details concerning the Δ current can be found in Ref. [13].

As alluded to in Section I, to ensure the translational invariance of the theory a lot of additional diagrams beyond the ones which are commonly included in the spectator approximation, are to be considered. These are the recoil diagrams where the photon couples to one of the recoiling particles or where an intermediate pion is exchanged with one or two non-detected nucleons. All diagrams which are included in our calculations are displayed in Fig. 4.

3. THE ^{4}HE(E, E′PP)NN AND ^{4}HE($\vec{\gamma}$, PP)NN RESULTS

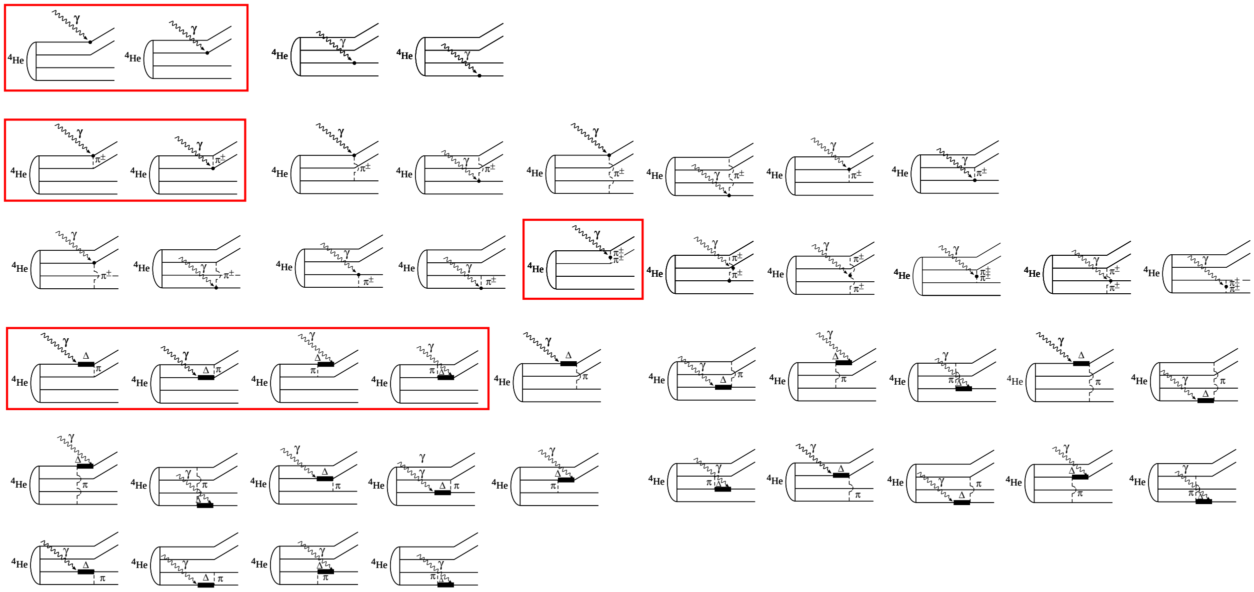

FIG. 4: Diagrams contributing to the ^{4}He($\gamma^{(*)}, NN$) process. The terms contained in the red boxes are the common diagrams included when adopting the spectator approximation. The others are recoil diagrams. The first row of terms corresponds with two-nucleon emission following electromagnetic coupling to the one-body current. The second and third row are related to the pion exchange diagrams while the last three rows contain the delta-current contributions.

As a general test of our model we tried to reproduce the available ^{4}He$(e,e'pp)nn$ data [3]. Fig. 5 displays the results of our plane-wave calculations. The difference between the harmonic oscillator and realistic calculations is attributed to the SRC effects. Moving to larger opening angles γ_{fq} implies probing higher relative momenta. The impact of the SRC amounts to shifting strength from the lower to the higher relative-momentum region. This translates itself in smaller (bigger) signals in the $(e,e'pp)$ cross sections at low (high) γ_{fq} opening angles. Most of the predicted $(e,e'pp)$ strength stems from the one-body current while the pion exchange and delta excitation contributions are almost negligible. Our predictions, though having a different tendency give the right order of magnitude for the cross section.

In the near future, ^{4}He$(\vec{\gamma},pp)nn$ data from the PIP-TOF collaboration will become available [4]. We calculated the ^{4}He$(\vec{\gamma},pp)nn$ cross section and photon asymmetry in QD-kinematics. This kinematical setup appears to be particularly well-suited to probe strongly correlated proton-proton pairs in the target nucleus. The results of the calculations are shown in Fig. 6. The cross section is dominated by the one-body current (blue curve) and reaches its maximum in so-called super-parallel kinematics. The green curve denotes the contribution from the delta current and reaches its maximum in the situation where both nucleons escape perpendicular to the transferred momentum. For two-proton knockout, pion-exchange diagrams can only contribute due the presence of the recoil diagrams. Indeed, the isospin dependence $(\vec{\tau}_1 \times \vec{\tau}_2)_z$ of these currents gives vanishing contributions when the spectator approximation is adopted. Our results indicate that the recoil diagrams are of minor importance for the computed (γ,pp) cross section. Our calculations confirm the general tendencies found by Laget [14]. His predictions for the $^3He(e,e'pp)n$ cross section are also characterized by the dominance of the one-body current in QD kinematics.

Although it appears that the recoil diagrams can be safely neglected when computing cross sections they have some effect on the polarization observables. The upper panel of Fig. 7 displays the photon asymmetry calculated with the complete set of diagrams, while for the lower panel only the diagrams in Fig.4 enclosed by red boxes are included (spectator approximation). Comparing both calculations one can conclude that the recoil diagrams alter the one-body, the pion exchange

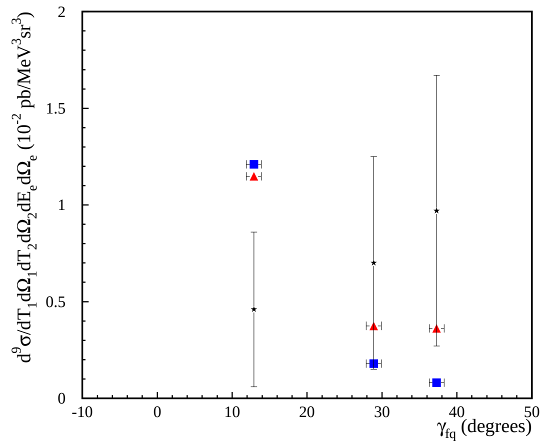

FIG. 5: The ^{4}He$(e, e'pp)nn$ cross section in coplanar and back-to-back kinematics plotted against the angle enclosed by the transferred momentum and the forward going proton. The transferred energy lies between 300 and 350 MeV, while the missing energy spans the interval [20 MeV, 60 MeV]. The blue squares are obtained with a harmonic oscillator wavefunction while the red triangles are the results of calculations on the basis of the realistic wave function of Eq. 1 including SRC effects. The black stars are data points from Ref. [3]

as well as the delta excitation contributions. The resulting photon asymmetry, however, is subject to rather small modifications when including the recoil diagrams.

4. CONCLUSIONS AND PROSPECTS

We have outlined a model for computing two-nucleon knockout cross sections on a ^{4}He target nucleus. Some early results of ^{4}He$(e, e'pp)nn$ and ^{4}He$(\gamma, pp)nn$ numerical calculations are presented. In all cases studied, the one-body current contribution produces the major contribution to the computed cross sections as well as to the polarization observables. Our investigations go beyond the spectator approximation and include all recoil diagrams. The recoil diagrams, which are needed to ensure the proper permutation symmetry of the scattering matrix and to make the model

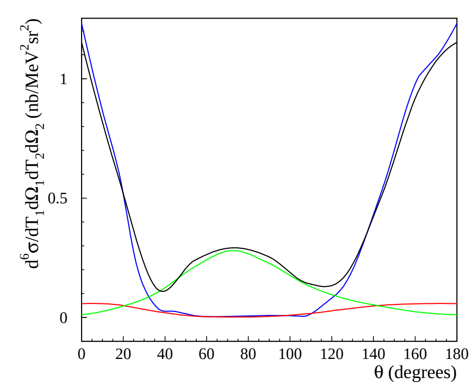

FIG. 6: The ^{4}He$(\gamma, pp)nn$-cross section in QD-kinematics ($P_m = 0$) as a function of the opening angle between the incoming photon and one of the outgoing protons. The transferred photon energy is 300 MeV. The curves show the contributions from the one-body current (blue curve), the pion exchange current (red curve), the delta excitation (green curve). The black curve is the total cross section.

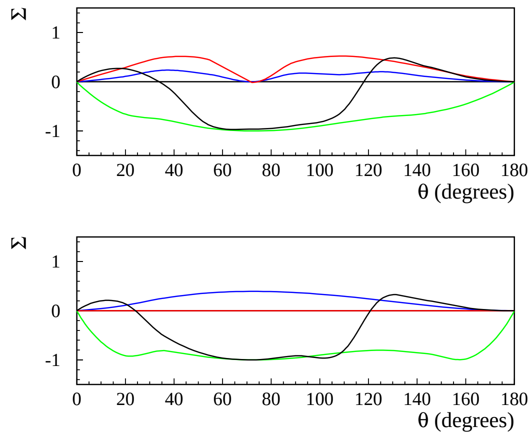

FIG. 7: The photon asymmetry for the ^{4}He$(\vec{\gamma}, pp)nn$-reaction in QD-kinematics at a photon energy of 300 MeV. Same line conventions as in Fig. 6. The upper panel displays the photon asymmetry calculated using the entire set of diagrams depicted in Fig. 4, while the graphs in the lower panel are obtained in the spectator approximation.

translationally invariant, modify the calculated two-nucleon knockout observables only marginally. The ^{4}He$(\vec{\gamma}, pp)nn$ and ^{4}He$(\vec{\gamma}, pn)X$ data which will become available in the foreseeable future will provide more testing grounds that should enable us to draw conclusions about the impact of SRC and recoil effects.

REFERENCES

[1] H. Kamada *et al.*, nucl-th/0104057
[2] J. Carlson and R. Schiavilla, Rev. Mod. Phys. **70** (1998) 743
[3] R. de Vries, PhD-thesis, Nikhef, Amsterdam (1995)
[4] F. A. Natter, PhD-thesis, Tübingen (2001) and T. Hehl, contribution to this proceedings.
[5] J.L Forest *et al.*, Phys. Rev. **C 54** (1996) 646
[6] L.M. Le Goff *et al.*, Phys. Rev. **C 50** (1994) 2278
[7] J.F.J. Van Den Brand *et al.*, Phys. Rev. Lett. **60** (1988) 2006
[8] C. Ciofi degli atti, E. Pace and G. Salmè, Phys. Rev. **C 43** (1991) 1155
[9] *http://www.phy.anl.gov/theory/research/rho1.gif*
[10] S. Boffi *et al.*, Electromagnetic Response of Atomic Nuclei, Axford Studies in Nuclear Physics (Clarendon Press, Oxford, 1996)
[11] J. Ryckebusch, D. Debruyne and W. Van Nespen, Phys. Rev. **C 57** (1998) 1319
[12] J. Ryckebusch, W. Van Nespen and D. Debruyne, Phys. Lett. **B 441** (1998) 1
[13] J. Ryckebusch *et al.*, Nucl. Phys. **A 624** (1997) 581
[14] J.M. Laget, Phys. Rev. **C 35** (1987) 832